

Evidence of Extreme Ultraviolet Superfluorescence in Xenon

L. Mercadier,^{1,2,*} A. Benediktovitch,³ C. Weninger,¹ M. A. Blessohl,⁴ S. Bernitt,^{5,4} H. Bekker,⁴ S. Dobrodey,⁴ A. Sanchez-Gonzalez,⁶ B. Erk,³ C. Bomme,³ R. Boll,³ Z. Yin,^{3,7} V. P. Majety,¹ R. Steinbrügge,⁴ M. A. Khalal,⁸ F. Penent,⁸ J. Palaudoux,⁸ P. Lablanquie,⁸ A. Rudenko,⁹ D. Rolles,^{3,9} J. R. Crespo López-Urrutia,⁴ and N. Rohringer^{1,3,10,†}

¹Max Planck Institute for the Structure and Dynamics of Matter, 22761 Hamburg, Germany

²European XFEL, 22869 Schenefeld, Germany

³Deutsches Elektronen-Synchrotron (DESY), 22607 Hamburg, Germany

⁴Max-Planck-Institut für Kernphysik, 69117 Heidelberg, Germany

⁵Institut für Optik und Quantenelektronik, Friedrich-Schiller-Universität Jena, 07743 Jena, Germany

⁶Department of Physics, Imperial College London, London SW7 2AZ, United Kingdom

⁷Max Planck für biophysikalische Chemie, 37077 Göttingen, Germany

⁸Laboratoire de Chimie Physique—Matière et Rayonnement, Université Pierre et Marie Curie, F-75231 Paris Cedex 05, France

⁹J. R. Macdonald Laboratory, Department of Physics, Kansas State University, Manhattan, Kansas 66506, USA

¹⁰Department of Physics, Universität Hamburg, 20355 Hamburg, Germany

 (Received 25 October 2018; revised manuscript received 22 May 2019; published 10 July 2019)

We present a comprehensive experimental and theoretical study on superfluorescence in the extreme ultraviolet wavelength regime. Focusing a free-electron laser pulse in a cell filled with Xe gas, the medium is quasi-instantaneously population inverted by $4d$ -shell ionization on the giant resonance followed by Auger decay. On the timescale of ~ 10 ps to ~ 100 ps (depending on parameters) a macroscopic polarization builds up in the medium, resulting in superfluorescent emission of several Xe lines in the forward direction. As the number of emitters in the system is increased by either raising the pressure or the pump-pulse energy, the emission yield grows exponentially over four orders of magnitude and reaches saturation. With increasing yield, we observe line broadening, a manifestation of superfluorescence in the spectral domain. Our novel theoretical approach, based on a full quantum treatment of the atomic system and the irradiated field, shows quantitative agreement with the experiment and supports our interpretation.

DOI: 10.1103/PhysRevLett.123.023201

Superfluorescence or superradiance is the spontaneous, collective decay of an extended, macroscopic ensemble of atoms that have been prepared in a population-inverted state, resulting in collimated, high-intensity radiation pulses. The pulses are emitted at a certain delay τ_D following excitation and have a duration that can be several orders of magnitude smaller than the typical upper-state lifetimes, often accompanied with temporal ringing. Superfluorescence has been first demonstrated in 1972 in the infrared [1], and later in the visible and microwave spectral regions [2]. Long before the advent of short-wavelength free-electron lasers (FELs), superfluorescence in optically thick media was proposed as a source for intense and pulsed extreme-ultraviolet (XUV) or x-ray radiation and has been theoretically examined [3–7]. Superfluorescence is closely connected to the physics of amplified spontaneous emission, superluminescence, and mirrorless lasing. In turn, the pulsed emission of a highly amplifying medium that is inverted impulsively in a single-pass geometry (gain-swept pumping) and that features large, transient gain is a manifestation of superfluorescence [2,6–9]. In this sense, strong x-ray $K\text{-}\alpha$ superfluorescence following ionization of the $1s$ shell with x-ray FEL (XFEL) pulses has been demonstrated in Ne gas [10,11], solid

copper [12], and manganese salts in aqueous solution [13]. In fact, theoretical modeling of the experiments in Ne [14] and a recent, refined theoretical analysis [15] clearly underline the superfluorescent character of this strongly amplified $K\text{-}\alpha$ emission. In the XUV region, superfluorescence following inner-shell ionization has so far not been demonstrated. The difficulty to obtain transient gain in the XUV region is a consequence of the disparate timescales of two competing processes: the very fast Auger decay on the fs (or Coster-Kronig decays on sub-fs) timescale limiting the lifetime of inner-valence vacancies and coherences, and the comparatively long (ns) radiative transition times. In the vacuum ultraviolet (VUV) regime, superfluorescence has been recently demonstrated in helium [16–19], following resonant excitation below the ionization threshold with an FEL.

Here, we present experimental and theoretical evidence for XUV superfluorescence of Xe gas. Population inversion is achieved by Auger pumping [4]: the rapid Auger decay following photoionization of the $4d$ shell with pulses of an XUV FEL creates a population inversion between the excited dicationic states that sustains coherent collective emission (see Fig. 1). Auger-pumped lasers have been experimentally realized in the 1980s in Xe

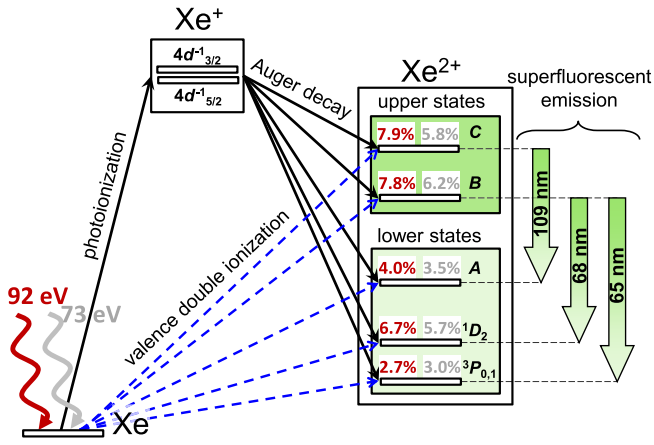


FIG. 1. Level scheme: The FEL pulse photoionizes the $4d$ shell of the Xe ground state. The resulting Xe^+ $4d^{-1}$ vacancies decay via Auger process into various Xe^{2+} and Xe^{3+} (not shown) states. Population inversion in Xe^{2+} is established between the upper (B , C) and lower (A , 1D_2 , and 3P_1) states of the observed transitions. Valence double ionization (dashed blue arrows) contributes to the population of the Xe^{2+} states. The population branching ratios of each state, relative to all Xe^+ , Xe^{2+} , and Xe^{3+} states as deduced from our coincidence measurements are given in red (gray) for $\omega_p = 92$ eV (73 eV). Since the 3P_1 and the 3P_0 are not experimentally resolved, the sum of the two ratios is shown.

and Kr gas [20,21] using a laser-generated plasma XUV source. Already then, it was speculated that the emission could stem from superfluorescence. The transverse pump geometry and the long rise time of the plasma-generated emission, however, were not ideal to sustain superfluorescence. FELs offer clear advantages: (i) their ultrashort pulses at high intensities guarantee a nearly instantaneous population inversion and (ii) their transverse coherence allows for tight focusing and gain-swept longitudinal pump geometry [5], which is ideal for superfluorescence [22]. Undoubtedly, a measurement of the temporal emission profile is the most straightforward way to characterize superfluorescence. Such a set-up is challenging and not available at the FLASH FEL, where our experiments have been performed. We, in turn, present spectroscopic evidence for XUV superfluorescence, which hitherto was hardly discussed in the literature [23–25]. Our experimental results are compared to our novel theory [15], which is fully quantized in both atomic and field degrees of freedom and goes beyond the typical phenomenological Maxwell-Bloch treatments [2,11,14]. In contrast to the recent demonstration of VUV super-radiance in resonantly pumped Helium [16–19], the incoherent pumping process of inner-shell ionization on the $4d$ giant resonance of this work can be achieved by optically pumped plasma sources [20,21,26] and thus has wider applicability. The study of coherent emission of Xe is of particular interest since it is electronically similar to tin—the target material for plasma-based sources for EUV lithography [27].

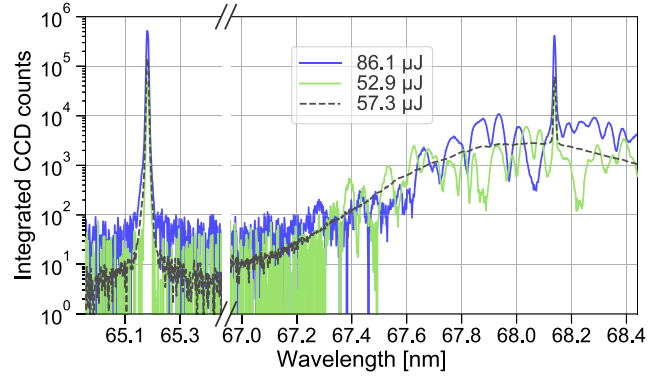


FIG. 2. Single-shot spectra (solid blue and green) and average over 725 spectra (dashed black) obtained with an FEL photon energy of $\omega_p = 73$ eV in 7 mbar of Xe. Two laser-like emission lines at 65.18 nm and 68.14 nm are observed. The typical SASE spectrum ($\Delta\omega_p \sim 1$ eV) of the FEL pulse appears in the fourth diffraction at around 68 nm $\hat{=} 73/4$ eV.

The experiment was performed at the CAMP end station of the FLASH FEL [28]. Pulses of ~ 80 – 100 fs duration at 10-Hz repetition rate were focused into a cell of pressurized Xe gas [10,11] creating a pencil-shaped pumped medium of 4.5 mm length and ~ 20 μm radius. The photon energy was tuned to 73 and 92 eV (below and on the giant $4d$ resonance [29]). The maximum available pulse energy on target was 90 μJ . The transmitted FEL pulse and the XUV emission were analyzed by a high-resolution spectrometer allowing the measurement of both the FEL spectrum and the superfluorescence lines in different diffraction orders. We observed intense XUV Xe emission in forward direction, with similar angular divergence to the pump FEL pulse, at (65.18 ± 0.20) nm, (68.14 ± 0.20) nm, (68.8 ± 0.2) nm, and (109.3 ± 0.5) nm. We attribute the latter one to the previously observed 108.9 nm line [20,30]. Examples of single shot and averaged Xe emission spectra are presented in Fig. 2, showing Xe emission lines at 65.18 and 68.14 nm as well as the FEL spectrum in the fourth diffraction order. The Xe level scheme is depicted in Fig. 1 [29,31–38]. Following $4d$ ionization, the states Xe^+ $4d_{3/2}^{-1}$ and $4d_{5/2}^{-1}$ rapidly decay by Auger process (lifetime ~ 6 fs [39]) to a manifold of different valence-excited Xe^{2+} states. This results in a population inversion between several pairs of states. States B ($5s^15p^5$ 1P_1) and C ($5s^05p^6$ 1S_0) serve as the upper states and A [$5s^25p^3$ (2D) $5d$ 1P_1], 1D_2 , and 3P_1 are the lower states of the observed transitions. Additionally, these dicationic states can be created by single-photon valence double ionization. Other transitions such as $C \rightarrow ^1D_2$, $B \rightarrow A$, or $C \rightarrow ^3P_1$ did not result in superfluorescence.

Our studies are focused on the strongest emission lines of 65.18 and 68.14 nm. In Fig. 3(a), the integrated intensity (yield) of the 65.18 nm Xe line is shown as a function of the FEL-pulse energy E_p for a photon energy of $\omega_p = 73$ eV (92 eV) at a pressure of 7 mbar (3.5 mbar)—the values maximizing the emission-line yield. A clear exponential

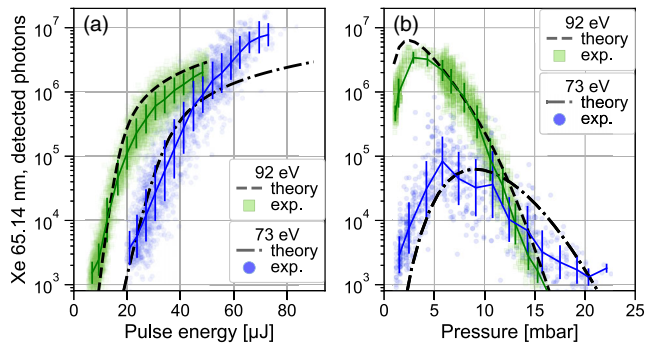


FIG. 3. Emission yield of the 65.18 nm line as a function of (a) FEL-pulse energy E_p for $\omega_p = 73$ eV (at 7 mbar Xe) and 92 eV (at 3.5 mbar Xe) and (b) pressure for fixed $E_p = 30$ μ J for $\omega_p = 73$ eV and $E_p = 75$ μ J for $\omega_p = 92$ eV. Symbols: Experimental single-shot data. For each data set, the solid line and error bars are the geometric mean and standard deviation, black lines are the result of the theory.

increase of the emission yield over four orders of magnitude results from varying E_p from 10 to 60 μ J. For $\omega_p = 92$ eV, the emission yield saturates for $E_p > 30$ μ J, while for $\omega_p = 73$ eV, saturation sets in for $E_p > 50$ μ J. The signal for $E_p \gtrsim 50$ μ J for $\omega_p = 92$ eV was saturated on the detector and is not shown. In the solid angle of emission ($\sim 10^{-5}$ sr), we calculate an exponential amplification factor of ~ 11 compared to the mere fluorescence signal. The pulse-to-pulse variation of the emission yield spreads over more than one order of magnitude for a given E_p , which was measured upstream from the interaction volume and transport optics. The scatter is due to measurement uncertainties of E_p as well as pointing instabilities of the FEL, leading to partial clipping of the FEL beam by the gas-cell apertures. The emission yield of the Xe 68.14 nm line shows a similar dependence on E_p , ω_p , and pressure (see the Supplemental Material [40] for additional data and the pulse-to-pulse correlation of emission yield of the 65- and 68-nm line). The large difference of gain between $\omega_p = 73$ eV and 92 eV is not only due to the difference in $4d$ photoionization cross sections ($\sigma_{\text{abs}} = 5.2$ Mb for 73 eV and $\sigma_{\text{abs}} = 25$ Mb for 92 eV [29,41]), but also due to differences in partial occupation rates of the upper and lower states of the emission lines (see Fig. 1), as revealed by our electron-electron coincidence measurements in Xe [40,42]: single-photon double ionization of the valence orbitals plays a significant role in the occupation of the superfluorescence states. At $\omega_p = 73$ eV, this pathway amounts to $\approx 15\%$ of the occupation of the upper state B , and $\approx 30\%$ of the lower states. At $\omega_p = 92$ eV its relative contribution is smaller. Valence double ionization de facto reduces the population inversion since this process tends to populate energetically lower lying Xe^{2+} states (see Fig. 1 and Table S-1 in the Supplemental Material [40]). For $\omega_p = 92$ eV, a conjugate shake-up Auger decay, which is energetically inaccessible at 73 eV [43], slightly enhances the population of the upper state of the 65- and 68-nm lines.

The pressure dependence of the emission yield is shown in Fig. 3(b). By increasing the pressure (and hence the number of emitters), the emission yield increases, saturates, and decreases for a fixed sample length. Saturation sets in for a pressure at which the attenuation length of the pump equals the sample length. Further increasing the pressure, a smaller and smaller fraction of the medium is inverted, and the rest of the medium absorbs the emitted photons, resulting in an exponential drop of the emission yield. The drop is more pronounced for $\omega_p = 92$ eV than for 73 eV because of the smaller absorption length of the pump FEL.

Insight into the collective emission process can be gained through our theoretical model [15,40]. The approach is based on a quantized treatment of both the emitted field and the atomic system and assumes a one-dimensional pump geometry. It enables us to capture the crossover from spontaneous emission through amplified spontaneous emission to superfluorescence. Although we are facing a complex level structure, we only consider a single transition. This approximation thus does not take into account the competition between two transitions sharing the same upper state, but should be sufficient for capturing the emission dynamics before the system saturates and Rabi oscillations occur [44]. The upper and lower level populations of this transition are prepared by an incoherent pump process, modeled within a rate equation approach (see the Supplemental Material [40] and Fig. 1 for cross sections and rates). Given the high FEL intensities, depopulation by sequential multiphoton ionization are included in the model for all involved levels, assuming cross sections for the neutral atom. Depending on the intensity on target, the FEL pulses (modeled as Gaussian temporal pulses of 80 fs FWHM) prepare the atoms in core-excited states on the time scale of 10–100 fs. The 15 ps travel time of the pump pulse through the cell is short compared to the long radiative lifetime ($1/\Gamma_{sp} \sim 1$ to 4 ns) of the upper lasing state. Thus, a prompt population inversion is established. Due to a separation of timescales (quasi-instantaneous pumping as compared to the collective superfluorescence time), the evolution of the atomic coherence is mainly determined by the interaction with the emitted electromagnetic field. Within our model we restrict ourselves to spontaneous emission as the sole decoherence effect: at the considered pressures and electron densities, electron collisions were not assessed as critical [20]. Doppler broadening alters the emission properties at the initial stages of amplification (see the Supplemental Material [40]) but is of minor importance in the observed regime of strong amplification [45].

The model solves for the ensemble averages of the occupation of the Xe ground state, the $4d^{-1}$ state and the emission levels as well as for the temporal and spectral properties of the outgoing radiation. It accounts for a nonresonant absorption of the emitted field. Fitting the

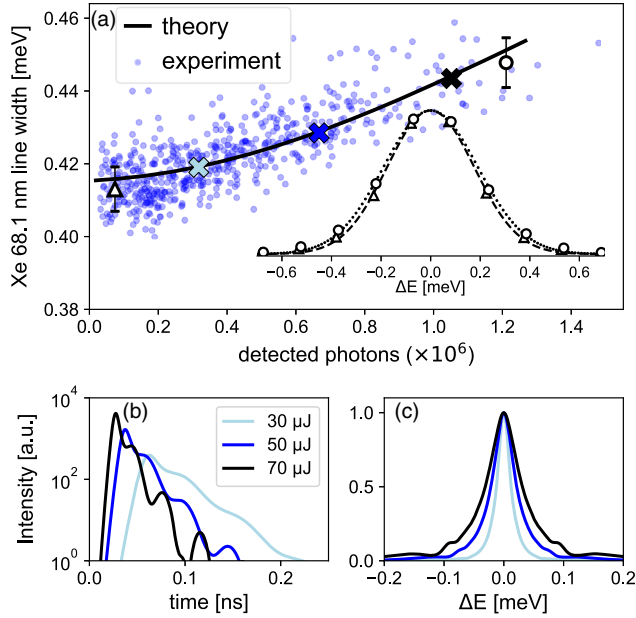


FIG. 4. (a) Measured line width of the Xe 68.14 nm emission line (FWHM of a Gaussian fit) as a function of emission yield for $\omega_p = 73$ eV. Each data point is obtained by accumulating three consecutive FEL pulses separated by $1 \mu\text{s}$. The error bars on the black triangle and circle show the standard deviation of the line width resulting from the fit. The corresponding normalized spectra (symbols) and fits (dashed and dotted lines) to these data points are shown in the inset. The black line is the theoretically determined line width taking into account the spectrometer resolution of 0.4 meV. The three points (colored crosses) mark the results of the theoretically determined temporal (b) and spectral (c) intensity profiles for various pump-pulse energies.

exponential drop of the emission yield at high pressures observed in Fig. 3(b), we estimate an absorption cross section of the 65.18 and 68.14 nm emission lines of $\sigma_{\text{abs}F} = 80$ Mb for $\omega_p = 92$ eV and $\sigma_{\text{abs}F} = 60$ Mb for $\omega_p = 73$ eV. Both values are within a factor of 2 from the absorption of neutral Xe [46]. Despite the limitations, the theory reproduces the trend of the emission yield as a function of pump energy [Fig. 3(a)] and pressure [Fig. 3(b)] for both $\omega_p = 73$ and 92 eV. To compare with the experiment, we assumed a total detection efficiency of 5%. For a quantitative comparison, a 2D treatment of the superfluorescence as well as a kinetic code following the evolution of the transient plasma and its opacity would need to be employed.

In the temporal domain, our theory reproduces the typical features of superfluorescence: Fig. 4(b) shows calculated time traces of the Xe 68.14 nm emission line for several pump-pulse energies at $\omega_p = 73$ eV. Increasing the pump-pulse energy from 30 to 70 μJ results in an effective increase of number of emitters from 2×10^9 to 4×10^9 , and a decrease in the delay times τ_D from 62 to 28 ps, along with a decrease of the pulse duration τ_W from

21 ps down to 7 ps. For 70 μJ (high within saturation), a ringing phenomenon is visible in the temporal intensity average. In comparison, for nanosecond plasma-based pump sources, Kapteyn *et al.* [21] measured pulse durations of the emission in the range of 600 to 1200 ps.

In the spectral domain, we measured a quasilinear broadening of the Xe 68.14 nm emission line as a function of its yield [Fig. 4(a)]. This broadening is at the limit of the resolution of our setup [47] and could only be observed in third diffraction order by integrating over 3 FEL pulses [see spectra in the inset of Fig. 4(a)]. The pressure in the cell was varied between 30 and 44 mbar. Figure 4(c) shows the spectral output of the theory. An increase of the pump-pulse energy and hence number of emitters results in a broader emission line and the emergence of shoulders. The spectral broadening corresponds to a decrease of the collective emission time (related to the width of the temporal peak τ_W), and the shoulders are an indication of the coherent temporal ringing in the spectral domain [40]. The theoretically determined width, convoluted with a 0.4 meV Gaussian response function to account for the spectrometer resolution, is shown as a black solid line in Fig. 4(a). While the shoulders are not resolved in the experiment, the theoretical line width quantitatively matches the experimentally observed trend. Thus, the measured line broadening with emission yield can be interpreted as an indication of superfluorescence.

In conclusion, we present experimental and theoretical data that underline the superfluorescent character of several Xe emission lines following 4d-shell ionization by an FEL and subsequent Auger decay. Notably, exponential growth of the emission yield as a function of pump-pulse energy is demonstrated in over four orders of magnitude, reaching saturation with more than 10^7 detected photons (10^8 to 10^9 emitted photons). The demonstration of saturation points towards the coherent nature of the emitted radiation. The line width shows an increase with the emission yield that is, within the experimental resolution, in agreement with our theoretical model. Collective emission times of the order of 10–100 ps are predicted and feature the typical ringing phenomenon. Compared to other sources, such as FELs or high brilliance table-top XUV lasers approaching the carbon 1s edge [48,49] with ps [50] and recently sub 100 fs [51] duration, the demonstrated XUV superfluorescence source is not competitive. Schemes could however be envisioned to shorten its pulse duration. Ionizing the upper lasing state with a short, time-delayed laser pulse would shrink the superfluorescence time, albeit at downscaled photon number. Coherent, optical quantum control schemes, such as recently suggested [52,53], could also be adapted to such a source. The fact that saturation can be reached with plasma sources [26] is very appealing. The high reproducibility of the emission wavelength of the Auger-pumped superfluorescence can deliver sharp spectral lines for diagnostics (for example photoelectron spectroscopy). An increase of the

emission yield can be achieved by optimizing the geometry of the gain medium, allowing for a larger number of emitters at higher solid angle [54]. Auger- and Coster-Kronig pumped systems have been theoretically studied for only a few atoms [55,56]. A systematic investigation of other atomic or molecular gain media could lead to more XUV emission wavelengths.

We acknowledge the technical and scientific teams at FLASH, in particular Dr. K. Tiedtke, Dr. A. Sorokin, and Dr. R. Treusch for their support during the experiment. We acknowledge the Max Planck Society for funding the development and the initial operation of the CAMP end-station within the Max Planck Advanced Study Group at CFEL and for providing this equipment for CAMP@FLASH. The installation of CAMP@FLASH was partially funded by the BMBF Grants No. 05K10KT2, No. 05K13KT2, No. 05K16KT3, and No. 05K10KTB from FSP-302. A.S.-G. is supported by the Science and Technology Facilities Council. A. R. and D. R. are supported by the Chemical Sciences, Geosciences, and Biosciences Division, Office of Basic Energy Sciences, Office of Science, U.S. Department of Energy, Grant No. DE-FG02-86ER13491. B. E., C. B., and D. R. also acknowledge support through the Helmholtz Young Investigator program. Z. Y. acknowledges financial support by SFB 1073, Project No. C02 from DFG. The coincidence experiments were performed at SOLEIL synchrotron; we are grateful to N. Jaouen and SEXTANTS team for help during the measurements, and to SOLEIL staff for stable operation of the storage ring. M. A. K. acknowledges the support of the Labex Plas@Par managed by the Agence Nationale de la Recherche, as part of the “Programme d’Investissements d’Avenir” under Reference No. ANR-11-IDEX-0004-02.

*laurent.mercadier@xfel.eu

†nina.rohringer@desy.de

- [1] N. Skribanowitz, I. P. Herman, J. C. MacGillivray, and M. S. Feld, Observation of Dicke Superradiance in Optically Pumped HF Gas, *Phys. Rev. Lett.* **30**, 309 (1973).
- [2] M. Gross and S. Haroche, Superradiance: an essay on the theory of collective spontaneous emission, *Phys. Rep.* **93**, 301 (1982).
- [3] J. C. MacGillivray and M. S. Feld, Criteria for x-ray superradiance, *Appl. Phys. Lett.* **31**, 74 (1977).
- [4] E. J. McGuire, Soft-X-Ray Amplified Spontaneous Emission via the Auger Effect, *Phys. Rev. Lett.* **35**, 844 (1975).
- [5] W. H. Louisell, M. O. Scully, and W. B. McKnight, Analysis of a soft-x-ray laser with charge-exchange excitation, *Phys. Rev. A* **11**, 989 (1975).
- [6] R. Bonifacio, F. A. Hopf, P. Meystre, and M. O. Scully, Steady-state pulses and superradiance in short-wavelength, swept-gain amplifiers, *Phys. Rev. A* **12**, 2568 (1975).
- [7] F. A. Hopf and M. O. Scully, Theory of an inhomogeneously broadened laser amplifier, *Phys. Rev.* **179**, 399 (1969).
- [8] F. A. Hopf, P. Meystre, M. O. Scully, and J. F. Seely, Coherence Brightening and Laser Lethargy in X-Ray Laser Amplifiers, *Phys. Rev. Lett.* **35**, 511 (1975).
- [9] V. Kocharovskiy, S. Cameron, K. Lehmann, R. Lucht, R. Miles, Y. Rostovtsev, W. Warren, G. R. Welch, and M. O. Scully, Gain-swept superradiance applied to the stand-off detection of trace impurities in the atmosphere, *Proc. Natl. Acad. Sci. U.S.A.* **102**, 7806 (2005).
- [10] N. Rohringer, D. Ryan, R. A. London, M. Purvis, F. Albert, J. Dunn, J. D. Bozek, C. Bostedt, A. Graf, R. Hill, S. P. Hau-Riege, and J. J. Rocca, Atomic inner-shell x-ray laser at 1.46 nanometres pumped by an X-ray free-electron laser, *Nature (London)* **481**, 488 (2012).
- [11] C. Weninger, M. Purvis, D. Ryan, R. A. London, J. D. Bozek, C. Bostedt, A. Graf, G. Brown, J. J. Rocca, and N. Rohringer, Stimulated Electronic X-Ray Raman Scattering, *Phys. Rev. Lett.* **111**, 233902 (2013).
- [12] H. Yoneda, Y. Inubushi, K. Nagamine, Y. Michine, H. Ohashi, H. Yumoto, K. Yamauchi, H. Mimura, H. Kitamura, T. Katayama, T. Ishikawa, and M. Yabashi, Atomic inner-shell laser at 1.5-ångström wavelength pumped by an x-ray free-electron laser, *Nature (London)* **524**, 446 (2015).
- [13] T. Kroll, C. Weninger, R. Alonso-Mori, D. Sokaras, D. Zhu, L. Mercadier, V. P. Majety, A. Marinelli, A. Lutman, M. W. Guetg *et al.*, Stimulated X-Ray Emission Spectroscopy in Transition Metal Complexes, *Phys. Rev. Lett.* **120**, 133203 (2018).
- [14] C. Weninger and N. Rohringer, Transient-gain photoionization x-ray laser, *Phys. Rev. A* **90**, 063828 (2014).
- [15] A. Benediktovitch, V. P. Majety, and N. Rohringer, Quantum theory of superfluorescence based on two-point correlation functions, *Phys. Rev. A* **99**, 013839 (2019).
- [16] M. Nagasono, J. R. Harries, H. Iwayama, T. Togashi, K. Tono, M. Yabashi, Y. Senba, H. Ohashi, T. Ishikawa, and E. Shigemasa, Observation of Free-Electron-Laser-Induced Collective Spontaneous Emission (Superfluorescence), *Phys. Rev. Lett.* **107**, 193603 (2011).
- [17] K. Nakajima, J. R. Harries, H. Iwayama, S. Kuma, Y. Miyamoto, M. Nagasono, C. Ohae, T. Togashi, M. Yabashi, E. Shigemasa, and N. Sasao, Simultaneous measurements of super-radiance at multiple wavelengths from helium excited states: I. Experiment, *J. Phys. Soc. Jpn.* **84**, 054301 (2015).
- [18] C. Ohae, J. R. Harries, H. Iwayama, K. Kawaguchi, S. Kuma, Y. Miyamoto, M. Nagasono, K. Nakajima, I. Nakano, E. Shigemasa *et al.*, Simultaneous measurements of superradiance at multiple wavelength from helium excited states: II. Analysis, *J. Phys. Soc. Jpn.* **85**, 034301 (2016).
- [19] J. R. Harries, H. Iwayama, S. Kuma, M. Iizawa, N. Suzuki, Y. Azuma, I. Inoue, S. Owada, T. Togashi, K. Tono, M. Yabashi, and E. Shigemasa, Superfluorescence, Free-Induction Decay, and Four-Wave Mixing: Propagation of Free-Electron Laser Pulses through a Dense Sample of Helium Ions, *Phys. Rev. Lett.* **121**, 263201 (2018).
- [20] H. C. Kapteyn, R. W. Lee, and R. W. Falcone, Observation of a Short-Wavelength Laser Pumped by Auger Decay, *Phys. Rev. Lett.* **57**, 2939 (1986).

- [21] H. C. Kapteyn and R. W. Falcone, Auger-pumped short-wavelength lasers in xenon and krypton, *Phys. Rev. A* **37**, 2033 (1988).
- [22] E. A. Sete, A. A. Svidzinsky, Y. V. Rostovtsev, H. Eleuch, P. K. Jha, S. Suckewer, and M. O. Scully, Using quantum coherence to generate gain in the XUV and X-ray: gain-swept superradiance and lasing without inversion, *IEEE J. Sel. Top. Quantum Electron.* **18**, 541 (2012).
- [23] M. G. Benedikt, A. M. Ermolaev, V. A. Malyshev, I. V. Sokolov, and E. D. Trifonov, *Super-Radiance: Multiatomic Coherent Emission* (Institute of Physics Publishing, Bristol and Philadelphia, 1996).
- [24] R. F. Malikov, V. A. Malyshev, and E. D. Trifonov, Shape of superradiation spectrum, *Opt. Spectrosc.* **51**, 225 (1981).
- [25] R. Malikov and E. Trifonov, Induced superradiance in activated crystals, *Opt. Commun.* **52**, 74 (1984).
- [26] M. H. Sher, J. J. Macklin, J. F. Young, and S. E. Harris, Saturation of the Xe III 109-nm laser using traveling-wave laser-produced-plasma excitation, *Opt. Lett.* **12**, 891 (1987).
- [27] V. Banine and R. Moors, Plasma sources for EUV lithography exposure tools, *J. Phys. D* **37**, 3207 (2004).
- [28] B. Erk, J. P. Müller, C. Bomme, R. Boll, G. Brenner, H. N. Chapman, J. Correa, S. Düsterer, S. Dziarzhytski, S. Eisebitt *et al.*, CAMP@FLASH: an end-station for imaging, electron- and ion-spectroscopy, and pump-probe experiments at the FLASH free-electron laser, *J. Synchrotron Radiat.* **25**, 1529 (2018).
- [29] U. Becker, D. Szostak, H. G. Kerkhoff, M. Kupsch, B. Langer, R. Wehlitz, A. Yagishita, and T. Hayaishi, Subshell photoionization of Xe between 40 and 1000 eV, *Phys. Rev. A* **39**, 3902 (1989).
- [30] H. Yamakoshi, P. R. Herman, M. P. L. Flohic, B. Xiao, L. Zhao, G. Kulcsar, F. W. Budnik, and R. S. Marjoribanks, Picosecond pumping of extreme-ultraviolet lasers using preformed laser plasmas, *J. Opt. Soc. Am. B* **13**, 436 (1996).
- [31] B. Kämmerling, B. Krässig, and V. Schmidt, Direct measurement for the decay probabilities of $4d_j$ hole states in xenon by means of photoelectron-ion coincidences, *J. Phys. B* **25**, 3621 (1992).
- [32] J. Jauhainen, H. Aksela, S. Aksela, A. Kivimäki, O. P. Sairanen, E. Nömmiste, and J. Végh, Correlation satellites in the Xe $N_{4,5}$ -OO and Kr $M_{4,5}$ -NN Auger spectra, *J. Phys. B* **28**, 3831 (1995).
- [33] N. Saito and I. H. Suzuki, Double auger probabilities from Xe $4d_j$, Kr $3d_j$, and Ar $2p_j$ hole states, *J. Phys. Soc. Jpn.* **66**, 1979 (1997).
- [34] T. Luhmann, C. Gerth, M. Groen, M. Martins, B. Obst, M. Richter, and P. Zimmermann, Final ion-charge resolving electron spectroscopy for the investigation of atomic photoionization processes: Xe in the region of the $4d \rightarrow \epsilon f$ resonance, *Phys. Rev. A* **57**, 282 (1998).
- [35] T. Carroll, J. Bozek, E. Kukkk, V. Myrseth, L. Sæthre, T. Thomas, and K. Wiesner, Xenon $N_{4,5}$ OO Auger spectrum—a useful calibration source, *J. Electron Spectrosc. Relat. Phenom.* **125**, 127 (2002).
- [36] P. Lablanquie, S. Sheinerman, F. Penent, R. I. Hall, M. Ahmad, T. Aoto, Y. Hikosaka, and K. Ito, Photoemission of threshold electrons in the vicinity of the xenon $4d$ hole: dynamics of Auger decay, *J. Phys. B* **35**, 3265 (2002).
- [37] J. Vieffhaus, M. Braune, S. Korica, A. Reinköster, D. Rolles, and U. Becker, Auger cascades versus direct double Auger: relaxation processes following photoionization of the Kr $3d$ and Xe $4d$, $3d$ inner shells, *J. Phys. B* **38**, 3885 (2005).
- [38] F. Penent, J. Palaudoux, P. Lablanquie, L. Andric, R. Feifel, and J. H. D. Eland, Multielectron Spectroscopy: The Xenon $4d$ Hole Double Auger Decay, *Phys. Rev. Lett.* **95**, 083002 (2005).
- [39] M. Jurvansuu, A. Kivimäki, and S. Aksela, Inherent lifetime widths of Ar $2p^{-1}$, Kr $3d^{-1}$, Xe $3d^{-1}$, and Xe $4d^{-1}$ states, *Phys. Rev. A* **64**, 012502 (2001).
- [40] See Supplemental Material at <http://link.aps.org/supplemental/10.1103/PhysRevLett.123.023201> for experimental details and a summary of the theory.
- [41] S. P. Shannon, K. Codling, and J. B. West, The absolute photoionization cross sections of the spin-orbit components of the xenon $4d$ electron from 70–130 eV, *J. Phys. B* **10**, 825 (1977).
- [42] M. A. Khalal, P. Lablanquie, L. Andric, J. Palaudoux, F. Penent, K. Bučar, M. Žitnik, R. Püttner, K. Jänkälä, D. Cubaynes, S. Guilbaud, and J.-M. Bizau, $4d$ -inner-shell ionization of Xe⁺ ions and subsequent Auger decay, *Phys. Rev. A* **96**, 013412 (2017).
- [43] T. Hayaishi, E. Murakami, Y. Morioka, H. Aksela, S. Aksela, E. Shigemasa, and A. Yagishita, Manifestation of Kr $3d$ and Xe $4d$ conjugate shake-up satellites in threshold-electron spectra, *Phys. Rev. A* **44**, R2771 (1991).
- [44] Cascading superradiant processes, such as FEL-induced multilevel superfluorescence in He [17–19], would need a more sophisticated level scheme.
- [45] Electron collisions and other sources of decoherence play a key role in the case of radiation from Xe clusters. This will be a major subject of a forthcoming paper on amplified spontaneous XUV emission of Xe Clusters.
- [46] J. Samson and W. Stolte, Precision measurements of the total photoionization cross-sections of He, Ne, Ar, Kr, and Xe, *J. Electron Spectrosc. Relat. Phenom.* **123**, 265 (2002).
- [47] Due to the limited resolution of 0.4 meV the measured broadening of the 68 nm line is on the scale of a few percent. The increase of the actual line broadening, however, is substantial, as can be seen from the theoretical simulations.
- [48] B. A. Reagan, M. Berrill, K. A. Wernsing, C. Baumgarten, M. Woolston, and J. J. Rocca, High-average-power, 100-Hz-repetition-rate, tabletop soft-x-ray lasers at sub-15-nm wavelengths, *Phys. Rev. A* **89**, 053820 (2014).
- [49] A. Rockwood, Y. Wang, S. Wang, M. Berrill, V. N. Shlyaptsev, and J. J. Rocca, Compact gain-saturated x-ray lasers down to 6.85 nm and amplification down to 5.85 nm, *Optica* **5**, 257 (2018).
- [50] Y. Wang, M. Berrill, F. Pedaci, M. M. Shakya, S. Gilbertson, Z. Chang, E. Granados, B. M. Luther, M. A. Larotonda, and J. J. Rocca, Measurement of 1 - ps soft-x-ray laser pulses from an injection-seeded plasma amplifier, *Phys. Rev. A* **79**, 023810 (2009).
- [51] A. Depresseux, E. Oliva, J. Gautier, F. Tissandier, J. Nejdil, M. Kozlova, G. Maynard, J. P. Goddet, A. Tafzi, A. Lifschitz *et al.*, Table-top femtosecond soft X-ray laser by collisional ionization gating, *Nat. Photonics* **9**, 817 (2015).

- [52] V. A. Antonov, Y. V. Radeonychev, and O. Kocharovskaya, Formation of ultrashort pulses via quantum interference between Stark-split atomic transitions in a hydrogenlike medium, *Phys. Rev. A* **88**, 053849 (2013).
- [53] T. R. Akhmedzhanov, V. A. Antonov, and O. Kocharovskaya, Formation of ultrashort pulses from quasimonochromatic XUV radiation via infrared-field-controlled forward scattering, *Phys. Rev. A* **94**, 023821 (2016).
- [54] J. C. MacGillivray and M. S. Feld, Limits of superradiance as a process for achieving short pulses of high energy, *Phys. Rev. A* **23**, 1334 (1981).
- [55] A. J. Mendelsohn and S. E. Harris, Proposal for an extreme-ultraviolet selective autoionization laser in Zn III, *Opt. Lett.* **10**, 128 (1985).
- [56] J. H. Krolik and P. R. Shapiro, Amplified spontaneous emission in the 1035 Å doublet of O^{5+} , *J. Phys. B* **16**, 4687 (1983).